FINITE VOLUME SOLUTION OF THE SHALLOW WATER EQUATIONS ON THE SPHERE

Janusz A. Pudykiewicz, Environment Canada, RPN, e-mail: Janusz.Pudykiewicz@ec.gc.ca

The finite volume discretization developed for the numerical approximation of the scalar conservation laws on a geodesic mesh described in [1] was extended to the shallow water equations on the sphere:

$$\frac{\partial \mathbf{v}}{\partial t} + (\zeta + f)(\mathbf{k} \times \mathbf{v}) = -\nabla\big(gh + \frac{\mathbf{v}\mathbf{v}}{2}\big), \quad \frac{\partial h^\star}{\partial t} + \nabla(h^\star \mathbf{v}) = 0, \tag{1}$$

where $\mathbf{v}$ is the velocity field on the sphere, ζ is the vertical component of the vorticity, f is the Coriolis parameter, $h^\star$ is the geopotential height, h_s is the surface height, $h = h_s + h^\star$, $\mathbf{k}$ is the unit vector normal to the sphere, and g is the gravity acceleration.

The system of equations (1) is discretized on a geodesic icosahedral grid composed of triangles with vertices located on the spherical surface (Fig. 1). The control volume, Ω_i, associated with the i^{th} node is created by a two step procedure. In the first step, the centers of the triangles and the mid-points of the edges are projected on the surface of the sphere. In the second step, Ω_i is defined as a polygon with the vertices located at the projected points (Fig. 2). The semidiscrete version of (1) can be written compactly in the following form:

$$\frac{d}{dt}\begin{pmatrix} \mathbf{u}_x \\ \mathbf{u}_y \\ \mathbf{u}_z \\ \mathbf{h}^\star \end{pmatrix} = \begin{pmatrix} -\mathbf{G}_x(g(\mathbf{h}^\star + \mathbf{h}_s) + \mathbf{U}) - \mathbf{W}_x + \nu\mathbf{D}^4\mathbf{u}_x \\ -\mathbf{G}_y(g(\mathbf{h}^\star + \mathbf{h}_s) + \mathbf{U}) - \mathbf{W}_y + \nu\mathbf{D}^4\mathbf{u}_y \\ -\mathbf{G}_z(g(\mathbf{h}^\star + \mathbf{h}_s) + \mathbf{U}) - \mathbf{W}_z + \nu\mathbf{D}^4\mathbf{u}_z \\ -\mathbf{D}_x(\mathbf{h}^\star\mathbf{u}_x) - \mathbf{D}_y(\mathbf{h}^\star\mathbf{u}_y) - \mathbf{D}_z(\mathbf{h}^\star\mathbf{u}_z) \end{pmatrix}, \tag{2}$$

where $\mathbf{u}_\eta$, $\mathbf{h}^\star$ are the vectors of the control volume average values of the velocity components and the geopotential height respectively ($\mathbf{u}_\eta = \{v_{\eta\,1}, \ldots, v_{\eta\,N}\}$, N is the number of control volumes), $\mathbf{W}_\eta = (\zeta + f)(\mathbf{k} \times \mathbf{v})_\eta$, $(\eta \equiv x, y, z)$, $\boldsymbol{\zeta} = \mathbf{Z}_x\mathbf{u}_x + \mathbf{Z}_y\mathbf{u}_y + \mathbf{Z}_y\mathbf{u}_y + \mathbf{f}_c$, $\mathbf{U}$ is the vector of grid cell averages of $v^2/2$, and ν is the hyperviscosity coefficient. The operators in (2) are defined by the following relations:

$$(\mathbf{D}_\eta\boldsymbol{\psi})_i = \sum_{j(i)}\left(\frac{1}{2}(\psi_i + \psi_{j(i)}) + \frac{L_{ij(i)}}{8}\big(\mathbf{h}^a_{ij(i)}\nabla_0^{(0.25,0.75)}\psi\big|_i - \mathbf{h}^b_{ij(i)}\nabla_0^{(0.25,0.75)}\psi\big|_{j(i)}\big)\right)\gamma^\eta_{ij(i)} \tag{3}$$

$$(\mathbf{G}_\eta\boldsymbol{\psi})_i = \sum_{j(i)}\left(\frac{1}{2}(\psi_i - \psi_{j(i)}) + \frac{L_{ij(i)}}{8}\big(\mathbf{h}^a_{ij(i)}\nabla_0^{(-0.75,0.75)}\psi\big|_i - \mathbf{h}^b_{ij(i)}\nabla_0^{(-0.75,0.75)}\psi\big|_{j(i)}\big)\right)\gamma^\eta_{ij(i)} \tag{4}$$

$$(\mathbf{Z}_\eta\boldsymbol{\psi})_i = \sum_{j(i)}\left(\frac{1}{2}(\psi_i + \psi_{j(i)}) + \frac{L_{ij(i)}}{8}\big(\mathbf{h}^a_{ij(i)}\nabla_0^{(0.25,0.75)}\psi\big|_i - \mathbf{h}^b_{ij(i)}\nabla_0^{(0.25,0.75)}\psi\big|_{j(i)}\big)\right)\omega^\eta_{ij(i)}, \tag{5}$$

where $\gamma^\eta_{ij(i)} = (n^{\eta\,(1)}_{ij(i)}\,\delta l^{(1)}_{ij(i)} + n^{\eta\,(2)}_{ij(i)}\,\delta l^{(2)}_{ij(i)})/S(\Omega_i)$, $\omega^\eta_{ij(i)} = (\tau^{\eta\,(1)}_{ij(i)}\,\delta l^{(1)}_{ij(i)} + \tau^{\eta\,(2)}_{ij(i)}\,\delta l^{(2)}_{ij(i)})/S(\Omega_i)$, $\nabla_0^{(\beta_1,\beta_2)}\psi\big|_i = \sum_{ij(i)}(\beta_1\psi_i + \beta_2\psi_{j(i)})\boldsymbol{\gamma}_{ij(i)}$, $\mathbf{n}^{(k)}_{ij(i)}$, $\boldsymbol{\tau}^{(k)}_{ij(i)}$, $(k = 1, 2)$ are the vectors normal and tangential to the segment of the boundary crossing the edge connecting points i and j(i), $\delta l^{(k)}_{ij(i)}$, $(k = 1, 2)$ are the lengths of the segments of the boundary, and $S(\Omega_i)$ is the measure of the control volume Ω_i (see Fig. 2).

The time integration of (2) can be performed with different Ordinary Differential Equations (ODE) solvers depending on the time step used in the calculation. In the initial stage system (2) was integrated using the standard 4-th order Runge–Kutta method with the time step selected to assure that the Courant number was limited by 1. The "l norms", mass conservation error and the normalized indicators of the minimum and maximum values for $h^\star$ for tests 1 and 2 (described in [2]) performed on a geodesic mesh with 40962 nodes are shown in the following table:

	l_1	l_2	l_∞	$\mathcal{M}$	$f_{\min}$	$f_{\max}$
test 1 ($\alpha = \pi/2$)	2.83×10^{-4}	9.25×10^{-4}	7.50×10^{-3}	0.0	-0.01	0.98
test 2 ($\alpha = 0$)	4.62×10^{-5}	6.68×10^{-5}	3.46×10^{-4}	0.0	-0.0002	1.00

REFERENCES

[1] Pudykiewicz J., 2006: Numerical solution of the reaction–advection–diffusion equation on the sphere. *J. Comp. Phys.*, **213**, 358.

[2] Williamson D. L., J. B. Drake, J. J. Hack, R. Jakob, and P. N. Shwartzrauber, 1992: A Standard Test Set for Numerical Approximations to the Shallow Water Equations in Spherical Geometry. *J. Comp. Phys.*, **102**, 211.

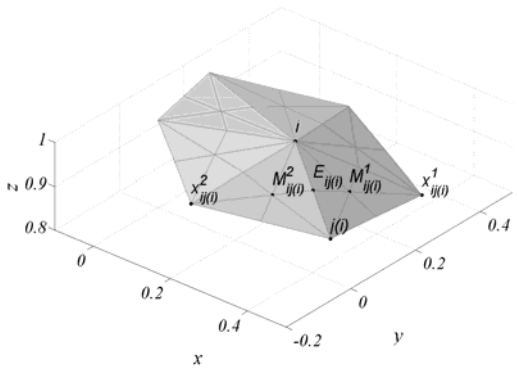

Fig. 1 Triangles used in the definition of the finite volumes on the sphere.

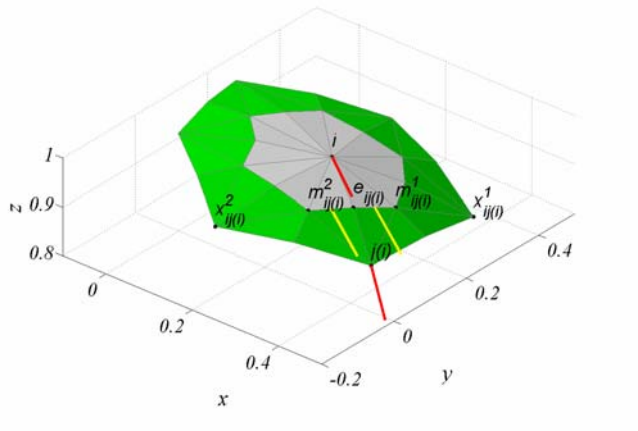

Fig. 2 The finite volume associated with a single node *i*.

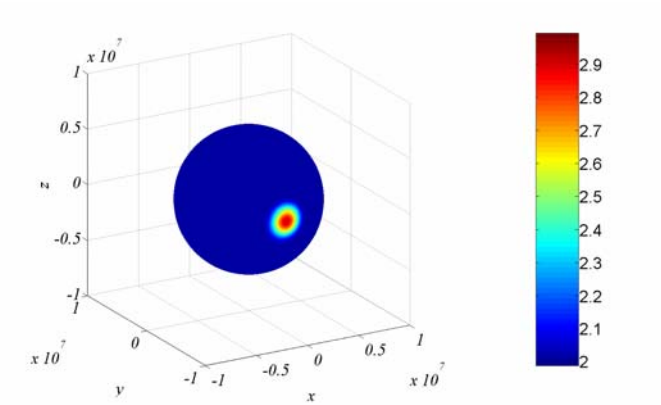

Fig. 3 Cosine hill after one rotation in flow crossing polar regions (test 1).

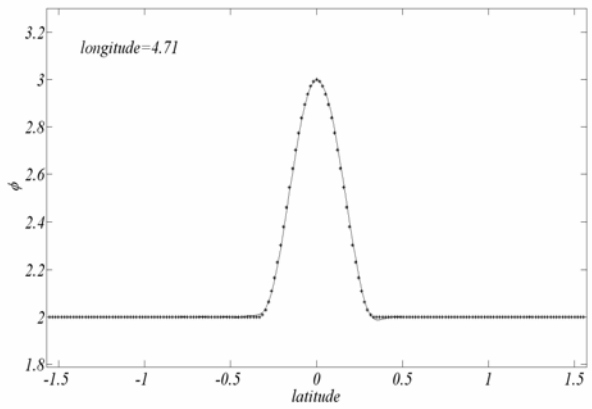

Fig. 4 Same as in Fig. 3 but the solution depicted by the solid line is that on the cross-section along the North-South plane (the analytical solution is represented by stars) .

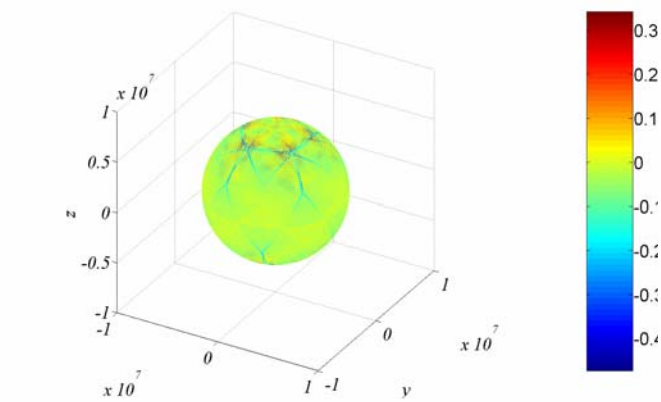

Fig. 5 The solution error for geopotential after 5 days for the global steady state nonlinear geostrophic flow (test 2).

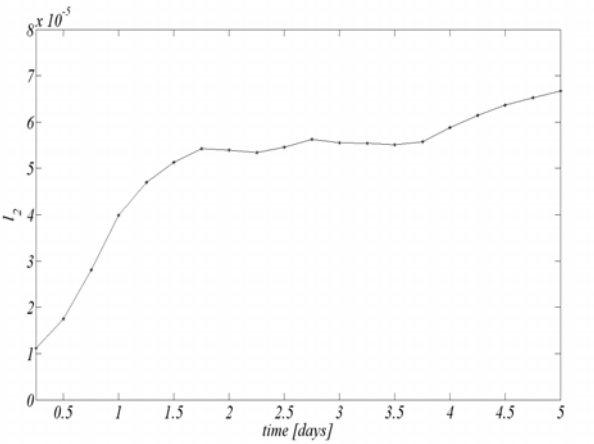

Fig. 6 The evolution of "l2" norm for the global steady state nonlinear geostrophic flow.